

Democratic temperature distribution and Local virial relation: Two hypotheses for self-gravitating systems

Y. Sota,^{1,2*} O. Iguchi^{1†}, M. Morikawa^{1‡} and A. Nakamichi^{3§}

¹ Department of Physics, Ochanomizu University, 2-1-1 Ohtuka, Bunkyo-ku, Tokyo, 112-8610, Japan

² Advanced Research Institute for Science and Engineering, Waseda University, Ohkubo, Shinjuku-ku, Tokyo, 169-8555, Japan

³ Gunma Astronomical Observatory, 6860-86, Nakayama, Takayama, Agatsuma, Gunma, 377-0702, Japan

15 March 2020

ABSTRACT

We propose two hypotheses which characterize the quasi-equilibrium state that realizes after the cold collapse of self-gravitating systems. The first hypothesis is the linear temperature-mass (TM) relation, which yields a characteristic non-Gaussian velocity distribution. The second hypothesis is the local virial (LV) condition, which, combining the linear TM relation, determines the unique mass density profile as $\rho(r) = \rho_0 r^{-4} e^{-r_0/r}$. This density profile is consistent with the data of cold collapse simulations and also with the data of observed surface brightness of a typical elliptical galaxy in the outer region. Two families of spherical and isotropic models, polytropes and King models, are examined from a view point of these two hypotheses. We found that the LV relation imposes a strong constraint on these models: only polytropes with index $n \gtrsim 4$ are compatible with the numerical results characterized by the two hypotheses among these models. King models with the concentration parameter $c \sim 2$ violate the LV relation while they are consistent with the $R^{1/4}$ law for the surface brightness. Hence the above characteristics can serve as a guideline to build up the models for the bound state after a cold collapse, besides the conventional criteria concerning the asymptotic behavior.

Key words: profiles: stellar dynamics – galaxies : kinematics and dynamics

1 INTRODUCTION

Collisionless self-gravitating systems (SGS) eventually settle down to a quasi-equilibrium state through the phase mixing and the violent relaxation processes under the potential oscillation (Lynden Bell 1967). This quasi-equilibrium state is a prototype of the astronomical objects such as galaxies and clusters of galaxies. These objects often show universal profiles in various aspects.

It would be true that the energy distribution function and the mass density distribution function are very appropriate to characterize SGS, and actually many studies have been done from this viewpoint. For example, the density profile is found to be $\rho \propto r^{-4}$ in spherical and cold collapses, *i.e.*, collapses with small initial virial ratio (Hénon 1964; Van Albada 1982) and $\rho \propto r^{-3} - r^{-4}$ in the cluster-pair merging processes (Merrall and Henriksen 2003).

On the other hand, the velocity distribution function

has not fully been examined so far despite its importance¹; anisotropy of velocity dispersion or lower moments of velocity distributions with respect to the deviations from Gaussian distributions have been mainly examined (e.g. Binney and Mamon 1982; Gerhard 1993). However, the full velocity distribution function plays an important role in identifying the quasi-equilibrium state, which should be properly characterized by the whole phase-space probability functions. Merrall *et al.* numerically showed that the velocity distributions in the central regions of the bound particles become Gaussian, when the bound particles are well relaxed (Merrall and Henriksen 2003). However, since SGS are manifestly non-additive systems (Nakamichi and Morikawa 2004), the ordinary Gaussian distribution would not be expected for the whole bound particles. Moreover, such non-Gaussian velocity distributions would be firmly connected

* E-mail: sota@cosmos.phys.ocha.ac.jp

† E-mail: osamu@phys.ocha.ac.jp

‡ E-mail: hiro@phys.ocha.ac.jp

§ E-mail: akika@astron.pref.gunma.jp

¹ So far, full velocity distributions have been mainly analyzed only for the line-of-sight velocity profiles because they can be directly compared with the observational data (Dejonghe 1987; Gerhard 1993)

with the density profile characteristic to SGS (Gerhard 1993; Kazantzidis et al. 2004).

Recently, we have simulated the self-gravitating N-body system by utilizing the leap-frog symplectic integrator on GRAPE-5, a special-purpose computer designed to accelerate N-body simulations (Kawai et al. 2000). When the system experiences violent gravitational processes such as cold collapse and cluster-pair collision, we obtained a universal velocity distribution profile expressed as the democratic (=equally weighted) superposition of Gaussian distributions of various temperatures (DT distribution hereafter) in which the local temperature $T(r)$ is defined using the local velocity variance $\langle v^2 \rangle$ as $T(r) := m\langle v^2 \rangle(r)/3k_B$, where m is the particle mass (Iguchi et al. 2004). Moreover, we have found that the locally defined temperature linearly falls down in the intermediate cluster region outside the central part, provided it is described against the cumulative mass M_r ; *i.e.*, $dT/dM_r = \text{const}$. This fact is consistent with the appearance of DT distributions.

Furthermore to the linear TM relation, we have also obtained another peculiar fact that the local virial relation between the locally defined potential energy and kinetic energy holds except for the weak fluctuations. More precisely, the local temperature $T(r)$ is proportional to the local potential $\Phi(r)$, with constant proportionality $6k_B T(r) = -m\Phi(r)$ for a wide class of cold collapse simulations. The bound region; *i.e.*, the region composed of the bound particles keeps this relation quite well at least during the time interval much longer than the initial crossing time. This is a prominent correlation in the phase space distribution function, and also constructs another backbone character of SGS after a cold collapse.

In sec.2 and 3, we will show that the above two backbone characteristics for SGS are supported by the results of a variety of cold collapse simulations. Then in sec.4, combining the two backbones, *i.e.*, the linear TM relation and the LV relation, we obtain a unique density profile $\rho(r) = \rho_0(r/r_0)^{-4} e^{-r_0/r}$ which asymptotically behaves as $\rho \propto r^{-4}$. Justification of this density profile will also be discussed. In sec.5 the above two backbone characteristics will be explored in two typical collisionless static models with spherical configuration and isotropic velocity dispersions; polytropes and King models. In sec.6 is denoted to the summaries and conclusions of this paper.

2 LINEAR TM RELATION

Let us now further consider the linear TM relation. In our recent work (Iguchi et al. 2004), we have examined the velocity distribution function of collisionless SGS after a cold collapse in numerical N-body calculations. According to this work, immediately after a cold collapse, well-relaxed and almost spherical-symmetric bound state is formed. In order to examine the local property, we use the cumulative mass M_r within the radius r ; *i.e.*, $M_r := 4\pi \int_0^r dr' r'^2 \rho(r')$ as a measure of the radial distance from the cluster center, which is defined as the position of the potential minimum. In our numerical simulation, we divide the whole system into several concentric shells with equal width in the coordinate M_r and consider the averaged quantities within each shell as local variables.

In our simulation, particles in the outermost region, which includes 20% of the total mass, escape almost freely just after the cold collapse and are irrelevant to the quasi-equilibrium state. Therefore we concentrate on the local temperature within the inner region initially including 80% of the total mass. More precisely, we define the bound particles as the particles inside the M_r , at which the local temperature $T(M_r)$ takes the minimum value. Hereafter, we pay our attention to the bound region composed of these bound particles. In the central part of this region, the two-body relaxation proceeds and the particles evaporate toward outside. Moreover, in this central region, the effect of cut-off ϵ proposed in numerical simulations cannot be ignored completely. Discarding this part from the bound region, we found, that the local velocity variance, *i.e.*, the local temperature linearly decreases to zero in the coordinate M_r ,

$$\langle v^2 \rangle(r) = \frac{3k_B T}{m} = c(M_{tot}(t) - M_r) \quad \text{or} \quad c = -\frac{3k_B}{m} \frac{dT}{dM_r}, \quad (1)$$

where c is a positive constant and $M_{tot}(t)$ is the total mass of the bound particles at t . $M_{tot}(t)$ is initially equal to 80% of the total mass but is gradually diminished, as several particles evaporate from the bound state.

Here we examined the deviation of TM relation from the linear relation (1) for a variety of simulations of cold collapse. For the estimate of the deviation, we first take the time-average for the velocity dispersion at each shell to derive the time-averaged $\langle v^2 \rangle$ -mass relation. Then we linearly fit it as (1) to derive $\langle v^2 \rangle_{fit}$ and subtract it from $\langle v^2 \rangle$. In Fig.1, the deviation normalized by $\langle v^2 \rangle$ at the half mass radius are depicted for several simulations. The deviations are very small and are less than 10 percent at each M_r for all of the simulations we examined. Hence, this result is quite robust against initial conditions provided the collapse is cold. Even for the case of cluster-pair collision, this linear relation is widely obtained.

3 LOCAL VIRIAL RELATION

Besides the linear TM relation, there is another backbone characteristic for SGS as we now argue. It is well known that the gravitationally bound system approaches a virialized state satisfying the condition

$$\overline{W} + 2\overline{K} = 0, \quad (2)$$

where \overline{W} and \overline{K} are, respectively, the averaged potential energy and kinetic energy of the whole bound system. This is a global relation that holds for the entire system, after the initial coherent motion fades out.

Here we define the locally averaged potential energy and kinetic energy inside the radius r , respectively as

$$\overline{W}_r := \frac{1}{2} \int_0^r \Phi(r') \rho(r') 4\pi r'^2 dr', \quad (3)$$

$$\overline{K}_r := \int_0^r \frac{\langle v^2 \rangle(r')}{2} \rho(r') 4\pi r'^2 dr', \quad (4)$$

where $\star(r')$ means the local object \star evaluated at r' .

Then we extend the virial relation (2) locally as

$$\overline{W}_r + 2\overline{K}_r = 0, \quad (5)$$

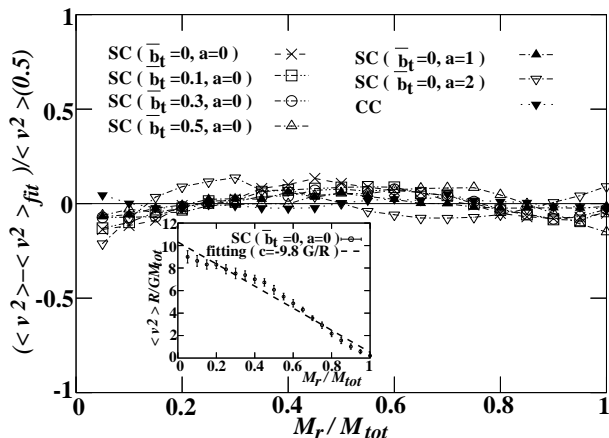


Figure 1. A mass dependence of velocity dispersion ($\langle v^2(M_r/M_{tot}) \rangle$) obtained by a typical cold collapse simulation; spherical collapse (SC) and cluster-pair collisions (CC). In the case of SC, 5000 particles are distributed with a power law density profile ($\rho \propto r^{-a}$) within a sphere of radius R and the initial virial ratio (\bar{b}_t) is set to be small. In the case of CC, each cluster has the equal number of particles (2500) and all particles are homogeneously distributed within a sphere of radius R and is set to be virialized initially. The initial separation of the pair is $6R$ along the x axis. In all of the simulations, softening length $\epsilon = 2^{-8}R$ is introduced to reduce the numerical error caused by close encounters. The inset figure shows that locally averaged velocity dispersion is plotted as a function of $M_r(t)/M_{tot}(t)$ for SC($\bar{b}_t = 0, a = 0$) as a typical example. Apparent linearity is remarkable. The solid line is the best fit line with $c = -9.8G/R$ (Eq.(1)). The open circles represent the time averaged numerical data from $t = 5t_{ff}$ and $t = 100t_{ff}$, where t_{ff} is the initial free fall time defined as $t_{ff} := \sqrt{R^3/GM_{tot}(0)}$. The deviation from the best fit line ($\langle v^2 \rangle_{fit}$) normalized by the velocity dispersion at the half mass is shown for some numerical simulations with different initial conditions. The value of each deviation is under 10%.

and examine how precisely this relation is locally attained inside a bound state.

More precisely, the above relation Eq.(5) is equivalent to the purely local relation

$$2\langle v^2 \rangle(r) = -\Phi(r), \quad (6)$$

at each position r . Hence, we define the LV ratio

$$b(r) := -2\langle v^2 \rangle(r)/\Phi(r), \quad (7)$$

and examine the value of $b(r)$ for each shell. For a wide class of collapses including cluster-pair collision examined in (Iguchi et al. 2004), the value $b(r)$ takes almost unity: it deviates from unity less than 10 percent upward in the intermediate region and a little more downward in the inner and outer region for all of the simulations (Fig.2). Hence a wide class of cold collapse simulations yield the relation (6) quite well. This LV relation should be another backbone characteristic of SGS, and this is our second hypothesis.

4 DENSITY PROFILE

We have explored the two hypotheses of SGS so far, *i.e.*, the linear TM relation Eq.(1) and the LV relation Eq.(6) for the

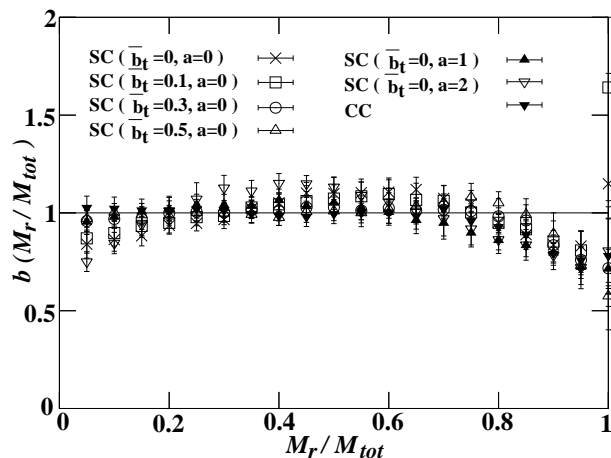


Figure 2. The LV relation for some numerical simulations with different initial conditions. The local virial ratio b is plotted as a function of M_r/M_{tot} . The initial condition of each simulation is the same as Fig.1. The virial ratios of each shell are time averaged from $t = 5t_{ff}$ and $t = 100t_{ff}$.

bound cluster. Combining these two relations, we now derive a mass density profile. We simply substitute Eq.(6) into Eq.(1) to obtain $2c(M_{tot} - M_r) = -\Phi$. Differentiating this by r and using Poisson's equation, we obtain a differential equation for the mass density $\rho(r)$:

$$\frac{d}{dr}(r^4 \rho) = \frac{G}{2c} r^2 \rho, \quad (8)$$

which admits the unique solution

$$\rho(r) = \rho_0 \left(\frac{r_0}{r} \right)^4 e^{-r_0/r}, \quad (9)$$

where $r_0 := G/2c$ and ρ_0 is a constant. This function well fits our numerical results (Fig.3). The asymptotic behavior $\rho(r) \propto r^{-4}$ is consistent with previous works (Jaffe 1987; Makino et al. 1990). However, the central part of this density is unphysical, since it increases with increasing radius r inside $r_* := r_0/4$. This fact warns that the two hypotheses we proposed are not always justified in the entire region.

The fact that the density behaves correctly in the outer region motivates us to improve the inner region by giving up one of the two hypotheses. In fact, this unphysical region of (9) can be removed by making a slight modification² of one of the two hypotheses in the inner region. For example, if the slope c becomes larger, the peak position r_* becomes smaller from the definition of r_0 . Hence by connecting the linear functions $T(M_r)$ with different slopes so as to make the inner slope steeper, we can shift the position of r_* toward a center (See AppendixA). From the definition of r_* for (A2) ($r_\beta/4$ in AppendixA, for example), we can also shift it by reducing b_f in (A2). In this case we can keep the slope of TM constant in a full region. In Fig.1 and Fig.2, the linearity of TM relation is realized in a full region on average, while LV relation seems to have a weak peak in the intermediate region. Hence the actual numerical results seem to follow the latter case, *i.e.*,

² As for the speculation that this is not only a technical manipulation but there exists a physical motivation, see the last section 6.

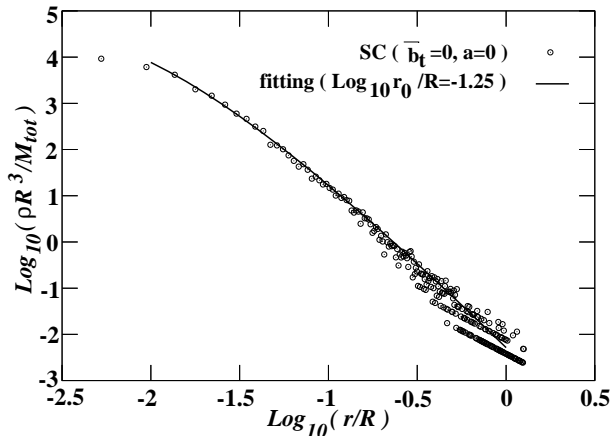


Figure 3. A log-log plot of a typical density profile after a cold collapse. The initial condition of this simulation is the same as SC ($\bar{b}_t = 0, a = 0$) in Fig.1. The open circles represent the numerical data at $t = 100t_{ff}$. The solid line is the density profile (Eq.(9)) with the best fit parameter ($\text{Log}_{10}(r_0/R) = -1.25$), which corresponds to $M_r|_{r=r_0}/M_{tot} \sim 0.43$.

the slight modification of the two hypotheses by reducing the local virial ratio b_f .

By combining these two procedures, we find that the density profile in the inner region is not strongly universal. On the other hand that in the outer region is universal and we have the asymptotic form $\rho \propto r^{-4}$ for density profile irrespective of the ways to change the density profile in the inner regions. The value of the parameter r_0 derived from the fitting of the profile (9) to the numerical result (Fig. 3) is roughly equal to $0.05R$ and it increases for the hinger value of the initial virial ratio \bar{b}_t .

As for the comparison with observations, supposing the constant M/L ratio, this density profile successfully reproduces the $R^{1/4}$ law, for the surface-brightness profile (de Vaucouleurs 1948). We compared the surface brightness calculated from our density profile to the observational data of the elliptical galaxy NGC3379, which follows the $R^{1/4}$ law very well (de Vaucouleurs 1979). Our profile fits well to the brightness data up to the one order of magnitude outside from the effective radius r_{eff} (defined as the radius having half the total luminosity inside it) (Fig.4). This result is plausible since the density profile which behaves as $\rho \propto r^{-4}$ in the outer region such as the profile (9) is known to fit well to $R^{1/4}$ law (Van Albada 1982).

5 COMPARISON WITH SPHERICAL AND ISOTROPIC STATIC MODELS

We have extracted the essence of cold collapses of SGS in the form of two hypotheses, *i.e.*, the linear TM relation Eq.(1) and the LV relation Eq.(6). How are they justified?

A collisionless self-gravitating system can be described by the Vlasov equation for the phase space distribution function $f(\vec{r}, \vec{v})$ in the mean field limit. Especially any function of the integral of motion can be a stationary solution of the Vlasov equation. Here we treat several collisionless static and spherical solutions of SGS and examine which class of solutions meet the two hypotheses we proposed.

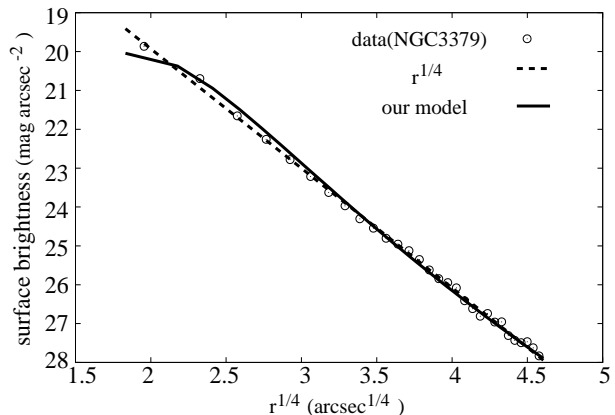


Figure 4. The surface brightnesses (mag arcsec^{-2}) are plotted against the fourth root of the radius. The open circles represent the observational data of NGC 3379, whose effective radius r_{eff} is about 56.42 arcsec (data set Pe4 of Table 2B in (de Vaucouleurs 1979)). The dashed line is the best fitted $R^{1/4}$ law. The solid line is the best fitted surface brightness calculated by use of the density profile (Eq.(9)) with the best fit parameter ($r_0^{1/4} = 2.8 \text{ arcsec}^{1/4}$), which corresponds to $1.09r_{\text{eff}}$.

It is well known that in a cold collapse, the velocity dispersion of bound system becomes radially anisotropic especially in outer regions (Van Albada 1982). On the other hand, in the paper (Iguchi et al. 2004), we take the average for the velocity dispersion for all of the components and get the results that TM relation becomes almost linear. Hence, our two hypotheses are irrelevant to an anisotropy of velocity dispersion, since we define the temperature as the averaged value.

Here, as zero-th order description, we regard the bound state as an isotropic system and compare it with the spherical and static model with an isotropic velocity dispersion described as $f(E)$, in terms of the particle energy per unit mass $E(r, v) := \Phi(r) + v^2/2$. Here we pay our attention to two sorts of solutions, polytropes and King models as the examples of those models.

First, we examined polytropes. Polytropes are the distribution functions with the form $f(r, v) = \epsilon(r, v)^{n-3/2}$, where ϵ is the relative energy defined as $\epsilon := -E + \Phi_*$, Φ_* is chosen so as to guarantee $f > 0$ for $\epsilon > 0$ and n is the polytropic index (Binney and Tremaine 1987). They have been examined in SGS N-body simulation in the context with Tsallis statistics (Taruya and Sakagami 2003). Polytropes with $n > 5$ necessitates a boundary to make the total mass finite since it diverges at infinity. Here, since we are interested in the case with no boundary, we focus our attention to the case with $n \leq 5$.

For polytropes with $n > 1/2$, it is easy to find that the local temperature $T(r)$ is connected to the local potential $\Phi(r)$ as,

$$\langle v^2 \rangle(r) = \frac{3k_B T}{m} = \frac{3}{1+n}(\Phi_* - \Phi(r)), \quad (10)$$

which is equivalent to

$$\frac{2\bar{K}_r}{\bar{W}_r} = \frac{6}{n+1} \left(\frac{M_r}{2\bar{W}_r} \Phi_* - 1 \right). \quad (11)$$

(See Appendix B for the derivation.) Since $\Phi_* = 0$ for

$n = 5$, the LV relation Eq.(5) or (6) is attained for $n = 5$, which means that the LV ratio (7) becomes unity for $n = 5$. This special solution with $n = 5$ can be analytically expressed as (C4) and is known as Plummer's model (Binney and Tremaine 1987). The TM relation of Plummer's model is obtained as (C7) and the slope dT/dM_r diverges as $M_r \rightarrow 0$. This discrepancy is plausible, since (9) is unphysical in the inner region. As is shown in appendix A, such discrepancies can be circumvented by shifting the inner slope as (A6), with maintaining the LV relation. In fact the TM relation of Plummer's model (C7) satisfies (A6) in the vicinity of $M_r = 0$.

In Fig.5, we depicted the LV ratio b as a function of M_r for $n < 5$ and obtained the result that b is almost unity and the local virial relation is attained well for $n \sim 5$. On the other hand for $n \sim 0.5$, b monotonically decreases with increasing M_r and deviates from the LV relation (6). As for the TM relation of polytropes, the slope becomes almost constant in the middle region from $0.2M_{tot} < M_r < 0.8M_{tot}$ and has a slight excess in the central region. However, the polytropes with larger n fail in keeping the TM relation in the outer region since $T(M_r)$ falls off steeply there (Fig.6). By contrast the polytrope with $n \sim 0.5$ keeps the constant slope of $T(M_r)$ up to the outer region. Recalling that the constant slope of TM relation up to the outer region is a key gradient for the DT distribution (Iguchi et al. 2004), the polytropes with $n \sim 5$ fail in reproducing the velocity distribution characteristic after a cold collapse. From (B3) and (C4), the mass density of Plummer's solution behaves as $\propto r^{-5}$ in the outer region. This is also inconsistent with the numerical results and with the behavior of (9). By contrast, the polytropes with $n \sim 0.5$ can reproduce DT distribution, although it strongly violates the LV relation in a bound region.

Secondly, we examined King models. King models have often been applied to fit the photometries of elliptical galaxies (e.g. Kormendy 1977; Bertin et al. 1988). They are conventionally analyzed with the concentration parameter $c := \log_{10}(r_t/r_c)$, where r_t and r_c are the tidal radius and the core radius, respectively (Binney and Tremaine 1987). It is shown that the King model with $c \sim 2.25$ fits the observational $R^{1/4}$ law quite well (Kormendy 1977). Here we examined the LV relation and the TM relation for the King models in the range $0.5 < c < 3.5$. For the family of such a parameter range, $b(M_r)$ becomes smaller in the central part for larger value of c , which means that the potential energy is locally more dominated than the kinetic energy in the central part. By contrast, for $c \sim 0.5$, the virial ratio becomes flat close to the center and takes the similar form to those of polytropes with $n \sim 5$ (Fig.7). As for the TM relation for King models, $T(M_r)$ for smaller value of c , especially $c \sim 0.5$, has the similar form as those of polytropes with $n \sim 5$. By contrast, for larger value of $c(\sim 2)$, $T(M_r)$ has an almost constant slope in the outer region (Fig.8). The density profile of King models in this parameter range behaves as $\rho \sim r^{-3} - r^{-4}$, which yields the surface density fitting well to the $R^{1/4}$ law. Hence King models with $c(\sim 2)$ follow the asymptotic behaviors of both T and ρ profile characteristic for the numerical results of cold collapse, although they violate the LV relation in the intermediate region.

Finally, we estimate the deviations from LV relation and linear TM relation for polytropes and King models more

quantitatively. Here we define the deviations from LV relation as $\delta_v := \sqrt{\langle (b-1)^2 \rangle}$ where $\langle \langle * \rangle \rangle$ denote the average of the functions of M_r defined as

$$\langle \langle * \rangle \rangle := \frac{1}{M_{tot}} \int_0^{M_{tot}} * dM_r. \quad (12)$$

For the definition of the deviation from linear TM relation, we first linearly extrapolate the function $T_e(M_r)$ as the form of $T_e(M_r) = AM_r + B$. Then we define the deviation as

$$\delta_t := \frac{\sqrt{\langle (T - T_e)^2 \rangle}}{T_{1/2}}, \quad (13)$$

where $T_{1/2}$ is the local temperature at the half mass radius. In the parameter range we examined, we plotted both δ_v and δ_t for polytropes and King models (Fig.9). We also calculated the δ_v s derived from the numerical simulations of cold collapse. They are obtained by averaging $(b(M_r/M_{tot}) - 1)^2$ at each M_r in the same way as the integral (12). We got the result that the δ_v derived from the simulations in Fig.1 and Fig.2 takes the value 0.106 ± 0.053 , which is depicted as the gray zone in Fig.9. The parameter range whose δ_v exceeds this gray zone is considered to be incompatible with the numerical simulations in Fig.2.

It is obvious that the δ_v almost vanishes for the polytropes $n \sim 5$, since $n = 5$ Plummer's model exactly satisfies the LV relation, but for n becomes small, δ_v becomes larger and exceeds the gray zone for $n \lesssim 3$ in Fig.9. Hence polytropes with $n \lesssim 3$ cannot follow the LV relation as well as the results of numerical simulations. On the other hand, the δ_t s for polytropes are almost constant for any parameter range $0.5 < n < 5$ and the value is almost 0.05. As for King models, the δ_v is larger than 0.1 for all of the parameter range and has a peak around $c = 2$. Especially, the δ_v of $1.6 \gtrsim c \gtrsim 2.9$ is larger than 0.2, which obviously exceeds the gray zone in Fig.9. This is in contrast to the fact that the surface brightness of King models fits well to $R^{1/4}$ law in this parameter range. On the other hand, the δ_t s of King models are less than 0.1 except for the high concentration case $c \gtrsim 3$. The strong deviation for $c \gtrsim 3$ is obvious, since the central temperature becomes much higher than those in the outer side for this parameter range.

In summary, we characterize a bound state after a cold collapse with (i)the LV relation (ii)the linear TM relation in the intermediate region and (iii)the linear TM relation in the outer region and the density profile which behaves as $\rho \sim r^{-4}$. Among these characteristics, the polytropes with $n \sim 5$ and the King models with $c \sim 2.0$ satisfy (i) and (ii) quite well but fail in (iii), while the polytropes with $n \sim 0.5$ and the King models with $c \sim 2.0$ satisfy (iii) very well but fail in (i) and (ii). From a viewpoint of the deviation from two hypotheses, the LV relation imposes a strong constraint for these models: only the polytropes with $n \gtrsim 4$ yield the δ_v less than the averaged value $\bar{\delta}_v$ (thick horizontal line in Fig.9). As for the TM relations, the deviations of these models are compatible with numerical results in almost all of the parameter ranges except for the high concentration cases in King models.

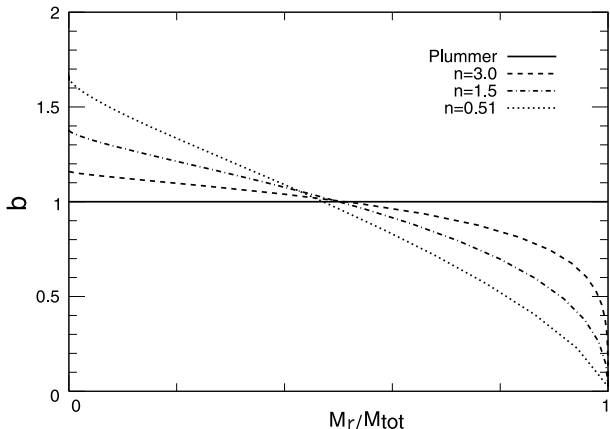


Figure 5. LV relation for polytropes. The solid curve refers to the LV ratio $b(M_r)$ as a function of cumulative mass M_r/M_{tot} for Plummer's model. The other curves refer to $b(M_r)$ for polytropes with $n = 3.0$ (dashed), $n = 1.5$ (dot-dashed), $n = 0.51$ (dotted).

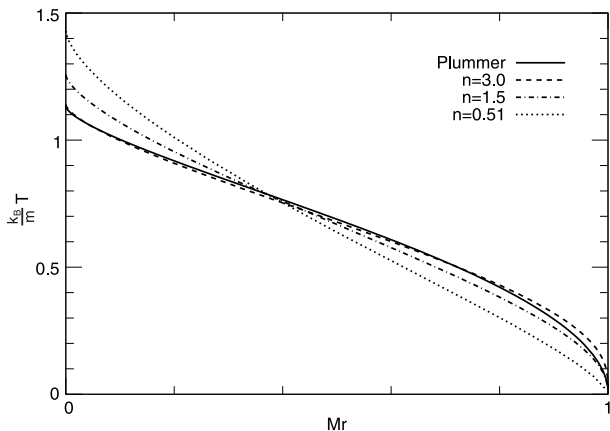


Figure 6. Temperature versus cumulative Mass (M_r) for polytropes. The solid curve refers to the local temperature $k_B T/m$ for Plummer's model (C7). The other curves refer to $k_B T/m$ for polytropes with $n = 3.0$ (dashed), $n = 1.5$ (dot-dashed), $n = 0.51$ (dotted). The units are those in which $G = M_{tot} = |E_{tot}| = 1$, where E_{tot} is the total energy of the system.

6 CONCLUDING REMARKS

In this paper, we have proposed (a) the linear TM relation and (b) the LV relation as the backbones of self-gravitating structures after a cold collapse. Based on these two hypothetical proposals, we have uniquely determined the mass density profile (9) in the quasi-equilibrium state.

Our density profile behaves as $r \sim r^{-4}$ in the outer region and fits well both to the data of cold collapse simulations and to the data of observed surface brightness of a typical elliptical galaxy. However, this density profile is unphysical in the inner region, where it decreases with the decreasing radius. We showed that such an unphysical region can be removed by modifying one of the two hypotheses as Appendix A inside the position of maximum density, r_* . The inner region of the bound state is, because of its high density, under the influence of the two-body relaxation caused by the close encounters of the particles. Hence, considering

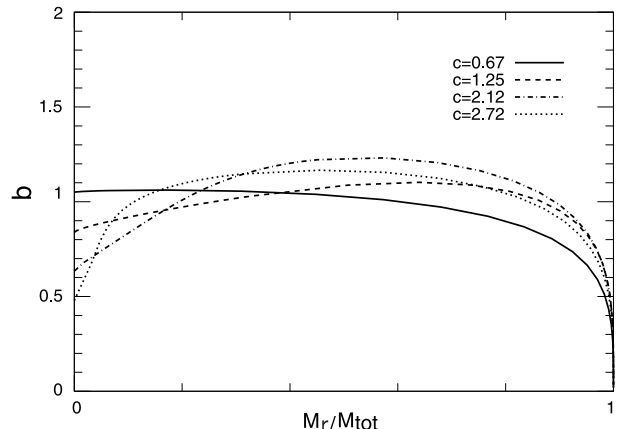


Figure 7. The same as Fig.5 but for King models. The solid curve refers to $b(M_r)$ for King model with $c = 0.67$. The other curves refer to $b(M_r)$ for King models with $c = 1.25$ (dashed), $c = 2.12$ (dot-dashed), $c = 2.72$ (dotted).

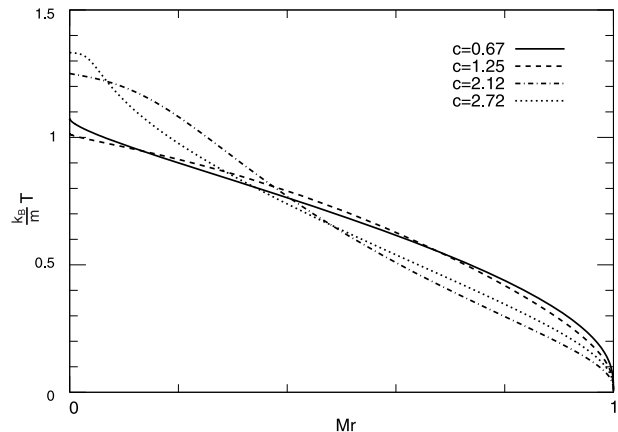


Figure 8. The same as Fig.6 but for King models. The solid curve refers to $k_B T/m$ for King model with $c = 0.67$. The other curves refer to $k_B T/m$ for King models with $c = 1.25$ (dashed), $c = 2.12$ (dot-dashed), $c = 2.72$ (dotted). The units are those in which $G = M_{tot} = |E_{tot}| = 1$.

that the bound states originate from a strong phase mixing after a cold collapse, we speculate that this modification in the inner region comes from the effect of the two-body relaxation on the collisionless bound state after a cold collapse. This speculation for the physical origin of the inner modification remains to be checked by numerical simulations or some theoretical techniques.

From a viewpoint of these two hypotheses, we compared our results with two isotropic static models. The polytrope with $n = 5$, Plummer's model is special among those models, since it exactly satisfies the LV relation. Moreover, the polytropes with $n \sim 5$ also satisfies the constant TM relation quite well in the intermediate region $0.2M_{tot} < M_r < 0.8M_{tot}$ except for the tiny excess in the inner region. On the other hand, both their TM relation and density profile in the outer region differ from the ones derived in cold collapse simulations: the temperature falls off more steeply and the density behaves as r^{-5} in the outer region. By contrast, the polytrope with $n \sim 0.5$ extends the linear TM relation

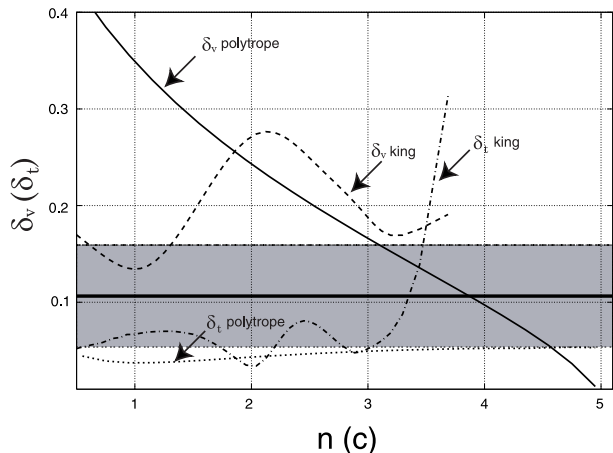


Figure 9. Deviation δ_v and δ_t versus model parameters for polytropes and King models. Residuals with respect to polytrope index n for polytropes and concentration parameter c for King models are plotted. Each curve refers to δ_v for polytropes (solid), δ_v for King (dashed), δ_t for polytropes (dotted), δ_t for King (dot-dashed). The gray zone refers to the range of $\delta_v = 0.106 \pm 0.053$ derived from the numerical simulations of cold collapse in Fig.1 and Fig.2. Thick horizontal line denotes $\delta_v = 0.106$.

up to the outer region, while it strongly violates the LV relation. The family of King models with small concentration parameter $c \sim 0.5$ yields the similar behavior as polytropes with $n \sim 5$. On the other hand, the family with higher $c \geq 2$ accepts neither of the two hypotheses in the inner region, although it yields in the outer region both the linear TM relation and the density profile with the asymptotic form $\propto r^{-4}$.

We also examined the deviations from the two hypotheses quantitatively for these models. Only the polytropes with $n \gtrsim 4$ are acceptable in that their deviations from both of the hypotheses are compatible with the numerical results of cold collapse. The LV relation imposes a strong constraint for these models. Especially for King models, the deviation from LV relation takes the maximum value around the parameter $c \sim 2$, in which the surface brightness fits well to $R^{1/4}$ law. This suggests that considering only the asymptotic behavior of the bound state is not enough to describe the collisionless static models to express observational or numerical results.

Combining the results for the above two models, we speculate that the models with a spherical symmetric configuration and with an isotropic velocity dispersion cannot follow all of the backbone hypotheses we proposed a) LV relation and b) linear TM relation. These models are mainly lack of the following properties of the bound states in the actual simulations of cold collapse: (i) deviation from a hydrostatic equilibrium state and (ii) anisotropy of velocity dispersion in the outer region.

As for (i), the hydrostatic equilibrium condition is not attained especially when the violent degree of the initial collapse is strong, since the bound state slowly expands outward and is not balanced with a gravitational force after a cold collapse. Hence, to express these conditions we may have to consider not the static solution but the stationary solution admitting the coherent motion of matters.

As for (ii), several collisionless static models with the anisotropic velocity dispersions or with the non-spherical symmetry have been proposed so far (Hénon 1973; Bertin and Stiavelli 1984; Stiavelli and Bertin 1985; Dejonghe 1987; Gerhard 1991; Bertin and Trenti 2003). However, physical origins of these models seem obscure, since most of them are motivated by just filling out the observational data such as $R^{1/4}$ law. The backbones we proposed are expected to be used as a guideline to build up the models following the characters of the bound states after a cold collapse. The generalization of polytropes with $n \gtrsim 4$ (Hénon 1973) seems promising since only these models, among those we have examined, satisfy both the backbone hypotheses. It also seems important how widely our two backbones are applicable in more general mixing processes including a merging process which yields a cuspy density profile in the central region (Navarro et al. 1996). These points are now under investigation.

ACKNOWLEDGEMENTS

We would like to thank Prof. Kei-ichi Maeda and Prof. Stefano Ruffo for the extensive discussions. All numerical simulations were carried out on GRAPE system at ADAC (the Astronomical Data Analysis Center) of the National Astronomical Observatory, Japan.

APPENDIX A: JOINT CONDITION FOR GENERALIZATION OF TM RELATION

Here we change the slope of TM relation at $r = r_j$ (or $M_r = M_{r_j}$) as

$$\langle v^2 \rangle = \begin{cases} \alpha M_r + \langle v^2 \rangle_0, & (r \leq r_j); \\ \beta (M_r - M_{r_j}) + \langle v^2 \rangle_j, & (r > r_j), \end{cases} \quad (\text{A1})$$

where both α and β are negative constant and $\langle v^2 \rangle$ is continuous at $r = r_j$. We also generalize the LV relation (6) as

$$2\langle v^2 \rangle(r) = -b_f \Phi(r), \quad (\text{A2})$$

using the constant value b_f .

By combining the relation (A1) with (A2), we can derive the differential equation for a mass density as

$$\frac{1}{r^2} \frac{d}{dr} (r^4 \rho) = \begin{cases} \frac{Gb_f}{2|\alpha|} \rho, & (r \leq r_j); \\ \frac{Gb_f}{2|\beta|} \rho, & (r > r_j). \end{cases} \quad (\text{A3})$$

The solution for each region of (A3) becomes

$$\rho = \begin{cases} \rho_\alpha \left(\frac{r_\alpha}{r}\right)^4 e^{-r_\alpha/r}, & (r \leq r_j); \\ \rho_\beta \left(\frac{r_\beta}{r}\right)^4 e^{-r_\beta/r}, & (r > r_j), \end{cases} \quad (\text{A4})$$

where $r_\alpha := \frac{Gb_f}{2|\alpha|}$ and $r_\beta := \frac{Gb_f}{2|\beta|}$.

From the continuity condition of ρ at $r = r_j$, the coefficient at each region needs to satisfy the condition,

$$\frac{\rho_\beta}{\rho_\alpha} = \left(\frac{r_\alpha}{r_\beta}\right)^4 e^{\frac{r_\beta - r_\alpha}{r_j}}. \quad (\text{A5})$$

Here we examine the case with $|\alpha| > |\beta|$, which leads to $r_\alpha < r_\beta$ and choose r_j so as to yield $r_j > r_\beta/4$. Then, since the outer solution takes the maximum value at $r_\beta/4$, we can

join the two solutions so as to $d\rho/dr < 0$ for $r > r_j$. The joined density profile takes the maximum value at $r_* = r_\alpha/4$, which is smaller than $r_\beta/4$. Hence by joining the solution with steeper slope in the inner region, the position of the maximum density r_* becomes smaller than that in the case with an unique slope β in a full region. By repeating the process to join the solution with steeper slope in the inner region, we can shift the position of r_* toward a center as much as possible. As the limit of the differentiable function form of $T(M)$, this condition corresponds to

$$\frac{dT}{dM_r} < 0 \quad \text{and} \quad \frac{d^2T}{dM_r^2} > 0. \quad (\text{A6})$$

APPENDIX B: DERIVATION OF LV RELATION FOR POLYTROPES

Following (Binney and Tremaine 1987), we use the notation using the relative energy ϵ and relative potential ϕ defined as

$$\begin{aligned} \epsilon &:= -E + \Phi_*, \\ \phi &:= -\Phi + \Phi_*, \end{aligned} \quad (\text{B1})$$

respectively. For polytropes, using these notations, the distribution function is described as

$$f(\epsilon) = \begin{cases} \kappa_1 \epsilon^p, & (\epsilon \geq 0); \\ 0, & (\epsilon < 0), \end{cases} \quad (\text{B2})$$

For (B2), density ρ and temperature T are simply expressed as

$$\rho = c_n \phi^n, \quad (\text{B3})$$

$$\langle v^2 \rangle = \frac{3k_B T}{m} = \frac{3}{n+1} \phi, \quad (\text{B4})$$

where $n := p + \frac{3}{2}$ and $c_n = (2\pi)^{3/2} \frac{(n-3/2)!}{n!} \kappa_1$.

From (3) and (B1),

$$\overline{W}_r = \frac{M_r \Phi_*}{2} - 2\pi \int_0^R \phi \rho(r) r^2 dr. \quad (\text{B5})$$

From (4), (B5), and (B4),

$$\overline{K}_r + \frac{3}{n+1} \overline{W}_r = \frac{3}{2(n+1)} M_r \Phi_*. \quad (\text{B6})$$

Especially for $n = 5$, from the condition $\Phi_* = 0$, the LV condition $2\overline{K}_r/|\overline{W}_r| = 1$ is obtained.

APPENDIX C: DERIVATION OF TM RELATION FOR PLUMMER'S MODEL

Following (Binney and Tremaine 1987), we define the dimensionless variables

$$\psi := \phi/\phi_0 \quad s := r/b, \quad (\text{C1})$$

where ϕ_0 is the value of the relative potential at the center and $b := \{4\pi G c_n \phi_0^{n-1}\}^{-1/2}$. Then, ψ is followed by Lane-Emden equation,

$$\frac{1}{s^2} \frac{d}{ds} \left(s^2 \frac{d\psi}{ds} \right) = \begin{cases} -\psi^n, & (\psi \geq 0); \\ 0, & (\psi \leq 0), \end{cases} \quad (\text{C2})$$

with the boundary condition

$$\lim_{s \rightarrow \infty} \psi(s) = \psi_*, \quad (\text{C3})$$

where $\psi_* := \Phi_*/\phi_0$. Especially for $n = 5$, the solution of (C2) with the flat boundary condition at the center becomes

$$\psi = \frac{1}{\sqrt{1 + s^2/3}}, \quad (\text{C4})$$

and meets the boundary condition

$$\lim_{s \rightarrow \infty} \psi(s) = \psi_* = 0. \quad (\text{C5})$$

In spherically symmetric case, the cumulative mass M_r is expressed as $M_r = -\frac{r^2}{G} \frac{d\phi}{dt}$, whose dimensionless form becomes

$$M_r = -s^2 \frac{d\psi}{ds}, \quad (\text{C6})$$

and the total mass M_{tot} is equal to $\sqrt{3}$. Substituting (C4) into dimensionless form of (B4) and (C6) and eliminating s , we can easily derive the TM relation of Plummer's model as

$$\frac{k_B T}{m} = \frac{1}{6} \sqrt{1 - \left(\frac{M_r}{M_{tot}} \right)^{2/3}}. \quad (\text{C7})$$

REFERENCES

- Bertin G. and Stiavelli M., 1984, ApJ, 137, 26
 Bertin G. and Trenti M., 2003, ApJ, 584, 729
 Bertin G., Saglia R. P. and Stiavelli M., 1988, ApJ, 330, 78
 Binney J.J. and Mamon G.A., 1982, MNRAS, 200, 361
 Binney J. J. and Tremaine S., Galactic Dynamics (Princeton University Press, Princeton, 1987).
 de Vaucouleurs G., 1948, Ann. d'Astrophys. 11, 247
 de Vaucouleurs G. and Capaccioli M., 1979 APJS 40, 699
 Dejonghe H., 1987, MNRAS, 224, 13
 Gerhard O. E., 1991, MNRAS, 250, 812
 Gerhard O. E., 1993, MNRAS, 265, 213
 Hénon M., 1964, Ann. Astrophys. 27, 83
 Hénon M., 1973, A&A 24, 229
 Iguchi O., Sota Y., Tatekawa T., Nakamichi A. and Morikawa M., 2004, astro-ph/0406600
 Jaffe W., 1987, Structure and Dynamics of Elliptical Galaxies, I.A.U.Symp. 127, 511
 Kawai A., Fukushige T., Makino J. and Taiji M., 2000, PASJ 52, 659
 Kazantzidis S., Magorrian J. and Moore B., 2004, ApJ, 601, 37
 Kormendy J., 1977, ApJ 218, 333
 Lynden Bell, 1967, MNRAS, 136, 101
 Makino J., Akiyama K., and Sugimoto D., 1990, PASJ 42, 205
 Merrall T.E.C. and Henriksen R.N., 2003, ApJ, 595, 43
 Nakamichi A. and Morikawa M., 2004, Physica A, 341, 215
 Navarro J. F., Frenck C. S. and White S. D. M., 1996, ApJ, 462, 563
 Stiavelli M. and Bertin G., 1985, MNRAS, 217, 735
 Taruya A. and Sakagami M., 2003, Phys. Rev. Lett 90, 181101
 Van Albada, 1982, MNRAS, 201, 939